arXiv:1002.3943v3 [cs.IT] 11 Oct 2011

Generalized Carrier to Interference Ratio Analysis for the Shotgun Cellular System in Multiple Dimensions

Prasanna Madhusudhanan*, Juan G. Restrepo†, Youjian (Eugene) Liu*, Timothy X Brown*+,
and Kenneth Baker+
*Department of Electrical, Computer and Energy Engineering,
†Department of Applied Mathematics, +Interdisciplinary Telecommunications Program
University of Colorado, Boulder, CO 80309-0425 USA
{mprasanna, juanga, eugeneliu, timxb, kenneth.baker}@colorado.edu

Abstract

This paper considers random cellular systems in one, two, or three dimensions. We study the carrier-to-interference ratio (CIR) and the carrier-to-interference-plus-noise ratio (CINR) at the mobile-station (MS), by using the so-called shotgun cellular system (SCS) model for the cellular system. In a SCS, the base-stations (BS) are placed randomly according to a non-homogeneous Poisson point process. For the SCS, analytical expressions for the tail probabilities of CIR and CINR are obtained. These results are generalized for an SCS affected by random shadow fading with any general distribution, for any arbitrary path-loss models, and for the MS located anywhere in the SCS. Further, for a special case of the SCS, namely, the homogeneous SCS, it is shown that the shadow fading has no effect on the CIR, and the effect of random transmission gains, power control, multiple channel reuse groups are analyzed. The techniques developed for the analysis of the CIR and the CINR holds applications beyond cellular networks and can be used to study several important scenarios in both uplink and downlink for cognitive radios, femtocell networks and other heterogeneous and multi-tier networks.

Index Terms

Cellular Radio, Co-channel Interference, Fading channels, Stochastic ordering.

I. INTRODUCTION

The modern cellular communication network is a complex overlay of heterogeneous networks such as macrocells, microcells, picocells, and femtocells. The base station (BS) deployment for these network can be planned, unplanned, or uncoordinated. Even when planned, the base station (BS) placement in a region deviates from a regular hexagonal grid due to site-acquisition difficulties, variable traffic load, and terrain. The coexistence of heterogeneous networks have further added to these deviations. As a result, the BS distribution appears increasingly irregular as the BS density grows and is outside standard performance analysis.

Two approaches of modeling have been widely adopted in the literature. At one end, the BSs are located at the centers of regular hexagonal cells to form an ideal hexagonal cellular system. At the other end, the BS deployments are modeled according to a Poisson point process which we denote a shotgun cellular system (SCS). In [1], the author makes a connection between these two models on a homogenous two dimensional (2-D) plane. It is shown that the carrier-to-interference ratio, $\left(\frac{C}{I}\right)$, of the SCS lower bounds that of the ideal hexagonal cellular system and moreover, the two models converge in the strong shadow fading regime. Since the BS deployment in the practical celluar system lies somewhere in between these two extremes, it is important to completely understand the performance of the SCS. Such an analysis holds significance in areas beyond cellular networks. Wireless LANs, cognitive radios, and ad-hoc networks are also characterized by irregular deployment of the BSs [2]–[13]. It is emphasized that, although the deployment of BSs in practice is not random, such a study is useful because it allows a thorough theoretical understanding of many important effects in the strong shadowing regime.

Recent work and our contributions: A Poisson point process has been adopted in the literature for the locations of nodes in the study of sensor networks, ad hoc networks and other uncoordinated and decentralized networks. In the case of ad-hoc networks, bounds on the transmission capacity are derived in several different contexts [7], [8], [11], [12], [14]–[18]. Finding the optimal bandwidth partitioning in uncoordinated wireless networks is considered in [19]. Similar outage probability analysis in ad-hoc packet radio networks is considered in [20], [21].

An underlying assumption in all the previous work is that the density of transmitters is constant throughout the cellular region, i.e. the Poisson point process is homogeneous. Such a model does not appropriately represent practical cellular networks where the BS distribution is irregular. In this paper, this scenario is incorporated by modeling the distribution of BSs by a non-homogeneous Poisson point process. Moreover, the region of interest need not be restricted to $\mathbb{R}^2$ as in prior work, and may be $\mathbb{R}^1$ or $\mathbb{R}^3$. Furthermore, the performance dependence on the MS location within the non-homogeneous cellular region is also characterized. Note that only the instantaneous $\frac{C}{I}$ at the MS are captured here. Handoff features and other dynamics are out of the scope of this work.

Finally, most research restricts the interference analysis to popular fading models like log-normal, Rayleigh, and Rician distributions and a propagation model that follows the inverse power law path-loss. Here, results are obtained that hold for any general fading distribution and arbitrary propagation models. This facilitates more accurately modeling the wireless network for analysing the signal quality at the desired receiver.

The following are the main contributions of this paper.

- A semi-analytical expression for the $\frac{C}{I}$ and $\frac{C}{I+N}$ distribution at the MS in a SCS with the propagation loss modeled by an inverse power law. (Sections III-A and IV)
- An accurate closed form approximation to the SCS $\frac{C}{I}$ distribution. (Section III-B)
- The SCS $\frac{C}{I}$ and $\frac{C}{I+N}$ distributions under shadow fading with any probability distribution (Section V), and for any arbitrary propagation loss model (Section VI).

Finally, in Section VII, applications of the results listed above in specific wireless communication networks are briefly described. In the following section, the system model is described and the performance metric of interest is defined. Further, the model is reduced to an equivalent Poisson point process in 1-D that is the basis of analysis in subsequent sections.

II. SYSTEM MODEL

This section describes the various elements used to model the cellular system, namely, the BS layout, the radio environment, and the performance metrics of interest. In the following subsection, we define SCS and introduce the terms associated with the BS layout in a SCS.

A. BS Layout

Definition 1. The *Shotgun Cellular System (SCS)* is a model for the cellular system in which the BSs are placed in a given l-dimensional plane (typically $l = 1, 2, \text{ and } 3$) according to a non-homogeneous Poisson point process on $\mathbb{R}^l$. The intensity function of the Poisson point process is called the BS density function in the context of the SCS.

In a practical cellular system, for places where the mobile user population is very small, the BSs are typically deployed along the highways. Such a cellular system can be modeled by a one-dimensional (1-D) SCS. . In the 1-D SCS, the BSs are placed according to a non-homogeneous Poisson point process with a BS density function $\lambda(r) \geq 0,$ where $r \geq 0$ is the distance of the BS from the origin on $\mathbb{R}^1$, such that the probability that a BS is placed in an interval $(r, r+h)$ of infinitesimal length h, is $\lambda(r)h$. The formal definition of the 1-D SCS incorporating the definition of the non-homogeneous Poisson point process is provided below.

Definition 2. A 1-D SCS with an average BS density function $\lambda(r),$ where $r \geq 0$ is the separation of the BS from the origin, is a counting process, $\{N(r),\ r \geq 0\}$, where $N(r)$ is the number of BSs upto a distance r from the origin, which satisfies

$N(0) = 0,$

$\{N(r),\ r \geq 0\}$ has independent increments,

$\mathbb{P}(\{1 \text{ BS in } (r, r+h)\}) = \lambda(r)h + o(h)$, and

$\mathbb{P}(\{0 \text{ BS in } (r, r+h)\}) = 1 - \lambda(r)h + o(h)$. [22]

Similarly, a two-dimensional SCS (2-D SCS) is a model for the planar deployment of BSs. Let every point on this 2-D plane be described by the polar coordinates (r, θ). In the 2-D SCS, the BSs are placed according to a non-homogeneous 2-D Poisson point process with a density function $\lambda(r, \theta),\ \forall\ r \geq 0,\ 0 \leq \theta \leq 2\pi$, which is the density of BSs about the origin in $\mathbb{R}^2$ at the point (r, θ), so that the probability that there exists a BS in an infinitisimal area $dA = rdrd\theta$ about the point (r, θ) is $\lambda(r, \theta)\, dA$.

Further, a three-dimensional SCS (3-D SCS) models the BS deployments in metropolitan areas, or wireless LANs (WLAN) in residential areas. If every point on the 3-D plane is described by the spherical coordinates (r, θ, ϕ), then the BS placement in the 3-D SCS takes place according to a non-homogeneous 3-D Poisson point process with a density function $\lambda\left(r, \theta, \phi\right), \ \forall \ r \geq 0, \ 0 \leq \theta \leq \pi, \ 0 \leq \phi \leq 2\pi$, which is the density of BSs about the origin in 3-D at the point (r, θ, ϕ), such that the probability that there exists a BS in an infinitisimal volume $dV = r^2 sin\theta dr d\theta d\phi$ about the point (r, θ, ϕ) is $\lambda\left(r, \theta, \phi\right) dV$.

A 1-D SCS in which $\lambda\left(r\right)$ is a constant everywhere on $\mathbb{R}^1$ is termed as a *homogeneous* 1-D SCS. Similarly, a 2-D/3-D SCS in which the respective density functions are a constant everywhere are termed as *homogeneous* 2-D/3-D SCS.

B. Radio Environment

In the SCS, all BSs are assumed to have identical transmission powers and antenna gains, and omni-directional antennas. The signal from the BS propagates through the wireless channel where it undergoes a deterministic path-loss, a random shadow fading and is affected by background noise. The path-loss is modeled by an inverse power law, and is proportional to $R^{-\varepsilon}$, where ε is the path-loss exponent, and R is the distance from the BS. The shadow fading factor is often modeled as a random variable with a log-normal distribution [23], [24]. The thermal and background noise in the system is given by a constant noise power N. Overall, the signal power at a distance R from the BS, accounting for both the path-loss and the shadow fading, is

$$P = K\Psi R^{-\varepsilon}, \tag{1}$$

where K captures the transmission power and the antenna gain of the BS, and Ψ is the random shadow fading factor.

C. Performance Metric

In this paper, we focus on the downlink performance of the SCS. In other words, we are concerned with the signal quality at a mobile-station (MS) within the SCS. The MS is without loss of generality located at the origin of the plane in which the SCS is defined, unless specified otherwise. The MS chooses to communicate with the BS that corresponds to the strongest received signal power. This BS is referred to as the "serving BS", and all the other BSs in the SCS are collectively called the "interfering BSs". Consequently, the signal quality at the MS is defined as the ratio of the received power from the serving BS $(C \text{ or } P_S)$ to the sum of the total interference power (I or P_I), and the noise power (N), and is called the carrier-to-interference-plus-noise ratio $\left(\frac{C}{I+N}\right)$. In an *interference limited system*, $I \gg N$ and the signal quality is the carrier-to-interference ratio $\left(\frac{C}{I}\right)$.

Using (1), the $\frac{C}{I}$ and $\frac{C}{I+N}$ at the MS are expressed as

$$\frac{C}{I} = \frac{K_S \Psi_S R_S^{-\varepsilon}}{\sum_{i=1}^{\infty} K_i \Psi_i R_i^{-\varepsilon}}, \quad \text{and} \quad \frac{C}{I+N} = \frac{K_S \Psi_S R_S^{-\varepsilon}}{\sum_{i=1}^{\infty} K_i \Psi_i R_i^{-\varepsilon} + N}, \tag{2}$$

where subscript S denotes the serving BS and subscript i indexes the interfering BSs; $K_S,\ \{K_i\}_{i=1}^{\infty}$ are independent and identically distributed (i.i.d) random variables; $R_S,\ \{R_i\}_{i=1}^{\infty}$ are random variables that come from underlying Poisson point process that govern the BS placement; $\Psi_S,\ \{\Psi_i\}_{i=1}^{\infty}$ are independent and identically distributed (i.i.d) random variables. Hence, $\frac{C}{I}$ and $\frac{C}{I+N}$ are random variables, and can be characterized by a probability density function (p.d.f.), cumulative density function (c.d.f.) or the tail probability. The tail probability of $\frac{C}{I+N}$ is given by $\mathbb{P}\left(\left\{\frac{C}{I+N} > \eta\right\}\right)$, and is the probability that a MS in the SCS has a signal quality of at least $\eta,\ \eta \geq 0$. Next, we characterize the tail probability of the $\frac{C}{I}$ at the MS in a SCS.

III. $\frac{C}{I}$ CHARACTERIZATION IN THE SCS

Here, the transmission power and the antenna gains of all the BSs in the SCS are assumed to be constant $(\text{say},\ K)$. Also, the shadow fading factors are assumed to be a constant. Hence, from the expression for $\frac{C}{I}$ in (2), the BS closest to the MS is the serving BS and the expression for $\frac{C}{I}$ can be equivalently written as

$$\frac{C}{I} = \frac{K R_1^{-\varepsilon}}{\sum_{i=2}^{\infty} K R_i^{-\varepsilon}}, \tag{3}$$

where $R_1 \leq R_2 \leq R_3 \cdots$ are distances between the BSs and the MS in a non-decreasing order.

In Section III-A, we first obtain the tail probability of $\frac{C}{I}$ for a MS at the origin of the 1-D SCS and illustrate the procedure to obtain the same when the MS is not located at the origin (refer Section III-A1) . Then, we obtain similar results for the 2-D and 3-D SCS by transforming them to an equivalent 1-D SCS (Section III-A2). In Section III-B, we focus on studying the $\frac{C}{I}$ and $\frac{C}{I+N}$ in the *homogeneous* 1-D, 2-D and 3-D SCS.

A. Tail probability of $\frac{C}{I}$

1) 1-D SCS: To obtain the tail probability of the $\frac{C}{I}$ at the MS in the 1-D SCS, we first present a theorem that derives the characteristic function of $\left(\frac{C}{I}\right)^{-1}$ at the MS. In order to state the theorem, we need the following definition.

Definition 3. A 1-D BS density function $\lambda(r),\ r \geq 0$ is said to be *stable* with respect to the path loss exponent ε if $\int_{s=0}^{r_1} \lambda(s)ds < \infty$ and $\lim\limits_{R_B \to \infty} \int_{r=r_1}^{R_B} \lambda(r) r^{-\varepsilon} dr < \infty,\ \forall\ r_1 > 0.$

Theorem 1. *In the 1-D SCS with a BS density function $\lambda(r)$ that is stable with respect to ε,*

(a) the characteristic function of P_I conditioned on R_1 is given by

$$\Phi_{P_I|R_1}(\omega|r_1) = \exp\left(\sum_{n=1}^{\infty} \frac{(i\omega K)^n}{n!} \int_{r=r_1}^{\infty} \lambda(r)\, r^{-n\varepsilon} dr\right), \text{ and} \tag{4}$$

(b) the characteristic function of $\left(\frac{C}{I}\right)^{-1}$ is given by

$$\begin{aligned}\Phi_{\left(\frac{C}{I}\right)^{-1}}(\omega) &= \mathrm{E}_{R_1}\left[\Phi_{P_I|R_1}\left(\frac{\omega}{P_S}\middle| R_1\right)\right] &(5)\\ &= \mathrm{E}_{R_1}\left[\exp\left(R_1 \times \int_{u=1}^{\infty} \left(\exp\left(i\omega u^{-\varepsilon}\right) - 1\right) \lambda(uR_1)\, du\right)\right], &(6)\end{aligned}$$

where $E_{R_1}[\cdot]$ is the expectation operator with respect to the random variable R_1.

Proof: See Appendix B. ■

The tail probability of $\frac{C}{I}$ may be directly obtained from the characteristic function and is

$$\mathbb{P}\left(\left\{\frac{C}{I} > \eta\right\}\right) = \begin{cases} \int_{\omega=-\infty}^{\infty} \Phi_{\left(\frac{C}{I}\right)^{-1}}(\omega) \left(\frac{1-\exp\left(-\frac{i\omega}{\eta}\right)}{i\omega}\right) \frac{d\omega}{2\pi}, & \eta > 0 \\ 1, & \eta = 0. \end{cases} \tag{7}$$

The above has been previously proved (See [25, Eq. (9)]).

Now, consider the problem of finding the tail probability of the $\frac{C}{I}$ at the MS in the 1-D SCS, but not located at the origin of the 1-D plane. Notice that $\lambda(r)$ has been defined as a density function w.r.t. the distance from the origin. When the BS density is defined for the entire 1-D plane $(d(x),\ -\infty < x < \infty)$, i.e. for either sides of the origin, the corresponding $\lambda(r)$ is

$$\lambda(r) \;=\; d(r) + d(-r),\ r \geq 0, \tag{8}$$

which is the sum of the densities of all the points that are at a distance r from the origin in the 1-D plane. This corresponds to $x = r$ and $x = -r$, respectively. The following lemma helps in finding the BS density as a function of distance from a MS at any point y on the 1-D plane.

Lemma 1. *Given an arbitrary density function* $d(x),\ -\infty < x < \infty$ *defined for the entire 1-D plane, and a MS at* y *on the 1-D plane,*

$$\lambda(r) \;=\; d(y-r) + d(y+r),\ r \geq 0 \tag{9}$$

is the density function as a function of the distance from the MS.

Proof: As in (8), $\lambda(r)$ is the sum of the densities of all the points that are at a distance r from the MS, and this corresponds to the points $y + r$ and $y - r$ in the 1-D plane. Hence, $\lambda(r)$ is given by (9). ■

Now, given $d(x),\ -\infty < x < \infty$, finding the tail probability of $\frac{C}{I}$ at the MS located at an aribitrary point y on the 1-D plane is a three step procedure. First, use Lemma 1 to find the equivalent $\lambda(r)$. Second, use $\lambda(r)$ in Theorem 1 to obtain $\Phi_{\left(\frac{C}{I}\right)^{-1}}(\omega)$, and thirdly, evaluate this function in (7) to obtain the desired result. The three step procedure now allows us to obtain the tail probability of the instantaneous $\frac{C}{I}$ at the MS which is anywhere along the 1-D SCS. Next, we show an interesting property of the $\frac{C}{I}$ at the MS in the 1-D SCS, for which we require the following definition.

Definition 4. Let X and Y be two random variables such that $\mathbb{P}\left(\{X > x\}\right) \leq \mathbb{P}\left(\{Y > x\}\right)$, $\forall\ x \in (-\infty, \infty)$, then X is said to be *smaller than* Y *in the usual stochastic order* and is given by $X \leq_{\text{st}} Y$. Also, $X =_{\text{st}} Y$ means $\mathbb{P}\left(\{X > x\}\right) = \mathbb{P}\left(\{Y > x\}\right),\ \forall\ x \in (-\infty, \infty)$. [26]

Corollary 1. *The p.d.f. (c.d.f and tail probability) of* $\frac{C}{I}$ *at the MS in the 1-D SCS with BS density function* $\lambda(r)$ *is the same as that in 1-D SCSs with BS density functions* $\frac{1}{a}\lambda(\frac{r}{a})$, $\forall\ a > 0$, *i.e.,* $\frac{C}{I}\big|_{\lambda(r)} =_{st} \frac{C}{I}\big|_{\frac{1}{a}\lambda(\frac{r}{a})}$.

Proof: Let $\{R_k\}_{k=1}^{\infty}$ correspond to the 1-D SCS with BS density function $\lambda(r)$.Then, since the ordered base station locations R_k's are determined by inter-base station distances, it follows that $\frac{C}{I}\big|_{\lambda(r)} \overset{(a)}{=} \frac{(aR_1)^{-\varepsilon}}{\sum_{k=2}^{\infty}(aR_k)^{-\varepsilon}}\Big|_{\lambda(r)} \overset{(b)}{=}_{\text{st}} \frac{\left(R_1'\right)^{-\varepsilon}}{\sum_{k=2}^{\infty}\left(R_k'\right)^{-\varepsilon}}\Bigg|_{\frac{1}{a}\lambda(\frac{r}{a})}$, where (a) is obtained by multiplying the numerator and denominator by $a^{-\varepsilon},\ a > 0$ in (3) and (b) follows from Appendix A-Lemma 3. Further, $\left\{R_k'\right\}_{k=1}^{\infty}$ in (b) correspond to 1-D SCS with BS density $\frac{1}{a}\lambda\left(\frac{r}{a}\right)$, $a > 0$. ■

As a result, $\left\{\frac{1}{a}\lambda\left(\frac{r}{a}\right),\ r \geq 0,\ a > 0\right\}$ forms a parametric family of BS density functions such that the 1-D SCSs corresponding to them have the same $\frac{C}{I}$ at the MS. In other words, appropriately scaling the BS density function will not change the p.d.f. of $\frac{C}{I}$. Next, we analyze the tail probability of $\frac{C}{I}$ at the MS in the origin of 2-D and 3-D SCS.

2) 2-D and 3-D SCS: Notice from the expression of $\frac{C}{I}$ in (3), that the distance of the BS from the MS is sufficient, and the additional details about the orientation of the BS in the 2-D or 3-D plane is irrelavant. Hence, for the study of the $\frac{C}{I}$, the 2-D and 3-D SCS can be transformed to an equivalent 1-D SCS using the following lemma.

Lemma 2. *(a) The distances of the BSs from the origin,* r, *in the 2-D SCS with a BS density function* $\lambda(r,\theta)$ *forms a Poisson point process with density function* $\lambda(r) = \int_{\theta=0}^{2\pi}\lambda(r,\theta)rd\theta,\ r \geq 0$, *provided the integral exists. Hence, for the* $\frac{C}{I}$ *analysis, the above 2-D SCS is equivalent to 1-D SCS with BS density function* $\lambda(r)$.

(b) The distances of the BSs from the origin, r, *in the 3-D SCS with a BS density function* $\lambda(r,\theta,\phi)$ *forms a Poisson process with density function* $\lambda(r) = \int_{\theta=0}^{\pi}\int_{\phi=0}^{2\pi}\lambda(r,\theta,\phi)r^2 sin\theta d\phi d\theta$, $r \geq 0$, *provided the integral exists. Hence, for the* $\frac{C}{I}$ *analysis, the above 3-D SCS is equivalent to 1-D SCS with BS density function* $\lambda(r)$.

Proof: Lemma $2(a)$ and $2(b)$ are a corollary of the Mapping theorem for Poisson processes in [27, Page 18], which says that the projections of a higher-dimensional Poisson processes are also Poisson processes. ■

Once the 2-D and 3-D SCSs have been translated to an equivalent 1-D SCS, the problem of finding the tail probability of $\frac{C}{I}$ is solved using the results in Section III-A1. Now, we focus on further studying the characteristics of $\frac{C}{I}$ at the origin of a *homogeneous* l-D SCS, $l = 1, 2, 3$.

B. Homogeneous l-D SCS

An important features of the homogeneous l-D SCSs is illustrated by the following lemma.

Corollary 2. *A homogeneous l-D SCS with a constant BS density λ_0 over the entire space is equivalent to the 1-D SCS with a BS density function $\lambda_l(r) = \lambda_0 b_l r^{l-1}, \ \forall\ r \geq 0$, where $b_1 = 2$, $b_2 = 2\pi$, $b_3 = 4\pi$.*

Proof: For the *homogeneous* 1-D SCS, the result follows from (8) with $d(x) = \lambda_0, \ \forall\ x$. For the *homogeneous* 2-D SCS and 3-D SCS, the result is obtained by evaluating the integrals in Lemma $2(a)$ and $2(b)$, respectively. ■

Notice in Corollary 2 that the BS density function of the equivalent 1-D SCS of the *homogeneous* l-D SCS is parameterized by λ_0 and l. Consider setting up Monte-Carlo simulations for the *homogeneous* l-D SCS for comparing the tail probability of $\frac{C}{I}$ as a function of λ_0. Figure 1 is the result of such an experiment and it shows that the tail probability does not vary as a function of λ_0. The following corollary warrants this empirical result.

Corollary 3. *In a homogeneous l-D SCS with a constant BS density λ_0, if the path-loss exponent satisfies $\varepsilon > l$,*

(a) the characteristic function of P_I conditioned on R_1 is given by

$$\Phi_{P_I|R_1}(\omega|r_1) \;=\; \exp\left(\frac{\lambda_0 b_l r_1^l}{l}\left(1 - {}_1F_1\left(-\frac{l}{\varepsilon}; 1 - \frac{l}{\varepsilon}; i\omega K r_1^{-\varepsilon}\right)\right)\right), \text{ and} \tag{10}$$

(b) the characteristic function of $\left(\frac{C}{I}\right)^{-1}$ is given by

$$\Phi_{\left(\frac{C}{I}\right)^{-1}}(\omega) = \mathrm{E}_{R_1}\left[\Phi_{P_I|R_1}\left(\frac{\omega}{P_S}\middle| R_1\right)\right] = \frac{1}{{}_1F_1\left(-\frac{l}{\varepsilon}; 1 - \frac{l}{\varepsilon}; i\omega\right)}, \tag{11}$$

where E_{R_1} is the expectation w.r.t. R_1, and ${}_1F_1(\cdot;\cdot;\cdot)$ is called the confluent hypergeometric function of the first kind (Refer [28, Chapter 1, Section 1.7] for the definition).

Proof: Using Corollary 2, the density function of the equivalent 1-D SCS is obtained, $\lambda(r) = \lambda_0 b_l r^{l-1}$. Next, by evaluating the integral in Theorem $1(a)$, (10) is obtained. Finally, using Fact 2 in Appendix A, compute the p.d.f. of R_1 to be $f_{R_1}(r_1) = \lambda_0 b_l r_1^{l-1} \exp\left(-\frac{\lambda_0 b_l}{l} r_1^l\right),\ 0 \leq r_1 \leq \infty$, using which the expectation in (11) can be evaluated to obtain the final result. ■

The significance of Corollary 3 is presented in the following two remarks.

Remark 1. The characteristic function of the $\left(\frac{C}{I}\right)^{-1}$ does not depend on λ_0, and hence the tail probability of $\frac{C}{I}$ at a MS in a homogeneous l-D SCS does not depend on λ_0.

Remark 2. The expression for the characteristic function of $\left(\frac{C}{I}\right)^{-1}$ for a *homogeneous* 2-D and 3-D SCS is same as of a *homogeneous* 1-D SCS with path-loss exponents $\frac{\varepsilon}{2}$ and $\frac{\varepsilon}{3}$, respectively.

Remark 1 proves why the curves corresponding to the *homogeneous* 1-D, 2-D and 3-D SCSs in Figure 1 are constant values. Remark 2 helps build an intuition of why the *homogeneous* 1-D SCS has a higher tail probability of $\frac{C}{I}$ than *homogeneous* 2-D and 3-D SCSs; Figure 1 now corresponds to comparing the tail probabilities of $\frac{C}{I}$ in a *homogeneous* 1-D SCS with path-loss exponents $\varepsilon,\ \frac{\varepsilon}{2},\ \text{and}\ \frac{\varepsilon}{3}$, respectively. As the path-loss exponent decreases, the BSs farther away from the MS have a greater contribution to the total interference power at the MS, and this leads to a poorer $\frac{C}{I}$ at the MS and a smaller tail probability.

In Figure 2, the tail probability of $\frac{C}{I}$ is plotted against ε; the squares $(\Box)$ and the pluses $(+)$ represent the values computed using (9) and Monte-Carlo simulations, respectively. The advantage of using (9) becomes evident when the path-loss exponent is arbitrarily close to 2 for the *homogeneous* 2-D SCS case, where the convergence of the Monte Carlo simulations is very slow and takes a large number of trials. An important corollary of Remark 2 is discussed below.

Corollary 4. *For a homogeneous l-D SCS, $l = 1, 2, 3 \cdots$, where the path-loss exponent is ε, the tail probability of $\frac{C}{I}$ at the MS is given by*

$$\mathbb{P}\left(\left\{\frac{C}{I} > \eta\right\}\right) = \mathbb{P}\left(\left\{\frac{C}{I} > 1\right\}\right) \times \eta^{-\frac{l}{\varepsilon}},\ \forall\ \eta \geq 1,\ \varepsilon > l \tag{12}$$

$$= \mathcal{K}_{\frac{\varepsilon}{l}} \eta^{-\frac{l}{\varepsilon}},\ \forall\ \eta \geq 1,\ \varepsilon > l, \tag{13}$$

where $\mathcal{K}_{\frac{\varepsilon}{l}}$ is a constant parameterized by $\frac{\varepsilon}{l}$.

Proof: In [1], we have shown that

$$\mathbb{P}\left(\left\{\frac{C}{I} > \eta\right\}\right) = \mathbb{P}\left(\left\{\frac{C}{I} > 1\right\}\right) \times \eta^{-\frac{2}{\varepsilon}}, \ \forall\ \eta \geq 1,\ \varepsilon > 2, \tag{14}$$

for a *homogeneous* 2-D SCS. From Remark 2, (14) holds for all *homogeneous* 1-D SCS with path-loss exponent $\frac{\varepsilon}{2}$ and therefore, for all *homogeneous* 3-D SCSs with path-loss exponent $\frac{3\varepsilon}{2}$. Hence, (12) hold true, and (13) is obtained by noting that the characteristic function of $\left(\frac{C}{I}\right)^{-1}$ is a function of $\frac{\varepsilon}{l}$ and so $\mathbb{P}\left(\left\{\frac{C}{I} > 1\right\}\right)$ is a constant parameterized by $\frac{\varepsilon}{l}$. ■

Recall that $\mathcal{K}_{\frac{\varepsilon}{l}}$ can be obtained by using (11) and evaluating the integral in (7) with $\eta = 1$. Note that $\frac{C}{I}$ is a non-negative random variable with a support of $[0, \infty)$, and surprisingly, its tail probability has such a simple form as given by (13) in the region $[1, \infty)$. Next, we define the so-called *few BS approximation* and derive closed form expressions for the tail probability of $\frac{C}{I}$ at MS in a *homogeneous* l-D SCS for both the regions $[0, 1)$ and $[1, \infty)$.

Definition 5. *The few BS approximation* corresponds to modeling the total interference power at the MS in a SCS as the sum of the contributions from the strongest few interfering BSs and an ensemble average of the contributions of the rest of the interfering BSs.

Recall from (3) that $P_I = \sum_{i=2}^{\infty} K R_i^{-\varepsilon}$, where $\{R_i\}_{i=1}^{\infty}$ is the set of distances of BSs arranged in the ascending order of their separation from the MS. The arrangement also corresponds to the descending order of their contribution to P_I, due to path-loss. In the few BS approximation, P_I is approximated by $\tilde{P}_I(k) = \sum_{i=2}^{k} K R_i^{-\varepsilon} + E\left[\left.\sum_{i=k+1}^{\infty} K R_i^{-\varepsilon}\right| R_k\right]$, for some k, where $E[\cdot]$ is the expectation operator and corresponds to the ensemble average of the contributions of BSs beyond R_k. The $\frac{C}{I}$ at the MS obtained by the few BS approximation is denoted by $\frac{C}{I_k}$.

Corollary 5. *For a homogeneous l-D SCS, with BS density λ_0 and $\varepsilon > l$, for k=1,2,3,$\cdots$*

$$E\left[\left.\sum_{i=k+1}^{\infty} K R_i^{-\varepsilon}\right| R_k\right] = \frac{\lambda_0 b_l K R_k^{l-\varepsilon}}{\varepsilon - l}. \tag{15}$$

Proof: Firstly, use Corollary 2 to reduce the SCS to the equivalent 1-D SCS with BS density function $\lambda(r) = \lambda_0 b_l r^{l-1},\ \forall\ r \geq 0$. Next, given k, use Fact 3 in Appendix A to divide the $[0, \infty)$

to non-overlapping intervals $[0, R_k]$ and (R_k, ∞), such that the events in them are independent of each other. Next, from Definition 2, the probability that there exists a BS in $(r, r+dr)$ is $\lambda(r)dr$. Hence, the ensemble average of the contribution a P_I due to BSs beyond R_k is the weighted sum of the contributions to P_I due to a BS in $(r, r+dr)$ for every $r \in (R_k, \infty)$ weighted by $\lambda(r)dr$. Hence, $E\left[\sum_{i=k+1}^{\infty} K R_i^{-\varepsilon} \middle| R_k\right] = \int_{r=R_k}^{\infty} K\lambda_0 b_l r^{-\varepsilon+l-1} dr$ and (15) is obtained. ■

Now, we present the theorem to obtain the tail probability of $\frac{C}{I_2} = \left.\frac{C}{I_k}\right|_{k=2}$ in closed form.

Theorem 2. *In a homogeneous l-D SCS with BS density λ_0 and path-loss exponent ε, satisfying $\varepsilon > l$, the tail probability of $\frac{C}{I_2}$ at the MS is given by*

$$\mathbb{P}\left(\left\{\frac{C}{I_2} > \eta\right\}\right) = \begin{cases} \eta^{-\frac{l}{\varepsilon}} C_{\frac{\varepsilon}{l}}, & \eta \geq 1 \\ 1 - e^{-u(\eta)}(1 + u(\eta)) + \eta^{-\frac{l}{\varepsilon}} D_{\frac{\varepsilon}{l}}(\eta), & \eta < 1 \end{cases}, \tag{16}$$

where $C_{\frac{\varepsilon}{l}} = G(0)$ and $D_{\frac{\varepsilon}{l}}(\eta) = G(u(\eta))$ with $G(a) = \int_{v=a}^{\infty} v e^{-v} \left(1 + v\left(\frac{\varepsilon}{l} - 1\right)^{-1}\right)^{-\frac{l}{\varepsilon}} dv$, and $u(\eta) \equiv \left(\frac{\varepsilon}{l} - 1\right)\left(\frac{1}{\eta} - 1\right)$.

Proof: Here we provide an outline of the proof. First, using Corollary 5, $\frac{C}{I_2} = \frac{K R_1^{-\varepsilon}}{\tilde{P}_I(2)}$, with $\tilde{P}_I(2) = K R_2^{-\varepsilon}\left(1 + \frac{\lambda_0 b_l}{\varepsilon - l} R_2^l\right)$. Next, notice that the event $\left\{\frac{C}{I_2} > \eta\right\}$ is equivalent to the joint event $\left\{R_1 \leq R_2,\ R_1 < \left(\frac{\eta \tilde{P}_I(2)}{K}\right)^{-\frac{1}{\varepsilon}}\right\}$ and thus, $\mathbb{P}\left(\left\{\frac{C}{I_2} > \eta\right\}\right) = \mathbb{P}\left(\left\{R_1 \leq \min\left(R_2, \left(\frac{\eta \tilde{P}_I(2)}{K}\right)^{-\frac{1}{\varepsilon}}\right)\right\}\right)$, where

$$\min\left(R_2, \left(\frac{\eta \tilde{P}_I(2)}{K}\right)^{-\frac{1}{\varepsilon}}\right) = \begin{cases} \left(\frac{\eta \tilde{P}_I(2)}{K}\right)^{-\frac{1}{\varepsilon}}, & \eta \geq 1 \\ \left(\frac{\eta \tilde{P}_I(2)}{K}\right)^{-\frac{1}{\varepsilon}}, & \eta < 1,\ R_2 > \left(\frac{l \times u(\eta)}{\lambda_0 b_l}\right)^{\frac{1}{l}} \\ R_2 & , \eta < 1,\ R_2 \leq \left(\frac{l \times u(\eta)}{\lambda_0 b_l}\right)^{\frac{1}{l}} \end{cases}.$$

Finally, (16) is obtained using the joint p.d.f., $f_{R_1,R_2}(r_1, r_2) = (\lambda_0 b_l)^2 (r_1 r_2)^{l-1} \exp\left(-\frac{\lambda_0 b_l}{l} r_2^l\right)$, $0 \leq r_1 \leq r_2 \leq \infty$, which results from Fact 1 and Fact 2 of Appendix A. ■

Notice that $\mathbb{P}\left(\left\{\frac{C}{I} > \eta\right\}\right) = \frac{K_{\frac{\varepsilon}{l}}}{C_{\frac{\varepsilon}{l}}} \mathbb{P}\left(\left\{\frac{C}{I_2} > \eta\right\}\right)$ for $\eta \geq 1$, and Figure 2 shows that the few BS approximation (●) closely follows the actual behavior (□). Figure 3 shows the comparison of the tail probabilities of $\frac{C}{I}$ (computed using the characteristic function of $\left(\frac{C}{I}\right)^{-1}$) and $\frac{C}{I_2}$ for a *homogeneous* 2-D SCS with path-loss exponent 4. Notice that the gap between the two tail probability curves is negligible in the region $\eta \in [0,1]$, and further, both the curves are straight lines parallel to each other in the region $\eta \in [1,\infty)$, when the tail probability is plotted against η, both in the logarithmic scale. This shows that the few BS approximation, is a good approximation for the actual $\frac{C}{I}$ and also characterizes the signal quality in closed form. Next, we use the results developed so far, to study the characteristics of $\frac{C}{I+N}$ at the MS in a SCS.

IV. $\frac{C}{I+N}$ CHARACTERIZATION IN A SCS

Without loss of generality, we study the $\frac{C}{I+N}$ at the MS in the 1-D SCS. We first obtain the tail probability of $\frac{C}{I+N}$ using the characteristic function of $\left(\frac{C}{I+N}\right)^{-1}$ derived in the following corollary.

Corollary 6. *In the 1-D SCS with a BS density function* $\lambda(r)$ *that is stable with respect to* ε*, the characteristic function of the sum of the total interference power* (P_I) *and noise power* (N) *conditioned on* R_1 *is* $\Phi_{P_I+N|R_1}(\omega|\, r_1) = \exp(i\omega N) \times \Phi_{P_I|R_1}(\omega|\, r_1)$*, and the characteristic function of* $\left(\frac{C}{I+N}\right)^{-1}$ *is* $\Phi_{\left(\frac{C}{I+N}\right)^{-1}}(\omega) = \mathrm{E}_{R_1}\left[\exp\left(i\frac{\omega}{P_S}N\right) \times \Phi_{P_I|R_1}\left(\frac{\omega}{P_S}\middle|\, R_1\right)\right]$, where $\Phi_{P_I|R_1}(\omega|\, r_1)$ is given by (4).

Proof: The expressions for $\Phi_{P_I+N|R_1}(\omega|\, r_1)$ and $\Phi_{\left(\frac{C}{I+N}\right)^{-1}}(\omega)$ follow directly from the definition of characteristic function, where N is a constant. ■

Further, the tail probability of $\frac{C}{I+N}$ is

$$\mathbb{P}\left(\left\{\frac{C}{I+N} > \eta\right\}\right) = \begin{cases} \int_{\omega=-\infty}^{\infty} \Phi_{\left(\frac{C}{I+N}\right)^{-1}}(\omega) \left(\frac{1-\exp\left(-\frac{i\omega}{\eta}\right)}{i\omega}\right) \frac{d\omega}{2\pi}, & \eta > 0 \\ 1, & \eta = 0. \end{cases} \tag{17}$$

and is obtained by substituting $\frac{C}{I}$ with $\frac{C}{I+N}$ in (7). Next, an interesting property of the $\frac{C}{I+N}$ at the MS in a *homogeneous* l-D SCS is given in the following corollary.

Corollary 7. *If the* $\frac{C}{I+N}$ *at the MS in a homogeneous* l*-D SCS is specified by* $(\lambda_0, \varepsilon, K, N)$ *where* λ_0 *is the constant BS density,* ε *is the path-loss exponent,* K *is transmission power and antenna* *gain of each BS, and N is the constant noise power, then,*

$$\left.\frac{C}{I+N}\right|_{(\lambda_0,\varepsilon,K,N)} =_{\text{st}} \left.\frac{C}{I+N}\right|_{\left(1,\varepsilon,1,N\lambda_0^{-\frac{\varepsilon}{l}}K^{-1}\right)}. \tag{18}$$

Proof: $\left.\frac{C}{I+N}\right|_{(\lambda_0,\varepsilon,K,N)} \overset{(a)}{=} \left.\frac{(\alpha R_1)^{-\varepsilon}}{\sum_{i=2}^{\infty}(\alpha R_i)^{-\varepsilon}+\frac{N}{(K\alpha^{\varepsilon})}}\right|_{\lambda_l(r)} \overset{(b)}{=}_{\text{st}} \left.\frac{K'\left(R_1'\right)^{-\varepsilon}}{\sum_{k=2}^{\infty}K'\left(R_k'\right)^{-\varepsilon}+N'}\right|_{\frac{1}{\alpha}\lambda_l\left(\frac{r}{\alpha}\right)}$, where $\alpha = \lambda_0^{\frac{1}{l}}$, $K' = 1$, $N' = N\left(K\alpha^{\varepsilon}\right)^{-1}$, (a) is obtained by expressing $\frac{C}{I+N}$ in terms of the equivalent 1-D SCS with $\lambda_l\left(r\right) = \lambda_0 b_l r^{l-1},\ r \geq 0$, and multiplying numerator and denominator with $\left(K\alpha^{\varepsilon}\right)^{-1}$, (b) follows from Corollary 1, and finally, (18) is obtained by noting that the 1-D SCS with BS density function $\frac{1}{\alpha}\lambda_l\left(\frac{r}{\alpha}\right)$ in (b) corresponds to a homogeneous l-D SCS with BS density 1. ■

So, it is sufficient to analyze a homogeneous l-D SCS with BS density $\lambda_0 = 1$ and maintain a lookup table for the tail probability of $\frac{C}{I+N}$ for different values of the noise powers and path-loss exponents using (17). The lookup table is presented for a homogeneous 2-D SCS in Figure 4 as a plot of $\mathbb{P}\left(\left\{\frac{C}{I+N} > 1\right\}\right)$ against noise powers for different values of path-loss exponents. Further, in a homogeneous l-D SCS with a high BS density λ_0, the equivalent SCS corresponds to a noise power $N' \to 0$ according to Corollary 7, in which case, $\frac{C}{I+N} \overset{D}{\to} \frac{C}{I}$, where $\overset{D}{\to}$ corresponds to the convergence in distribution. Hence, in an *interference-limited system* (large λ_0), the signal quality is measured in terms of $\frac{C}{I}$. In the following section, we study the effect of shadow fading on the $\frac{C}{I}$ and $\frac{C}{I+N}$ at the MS in the SCS.

V. SHADOW FADING IN A SCS

In [25], [29], we have shown that the $\frac{C}{I}$ at the MS is unaffected by shadow fading in a *homogeneous* 2-D SCS. Here, we present a theorem for obtaining the tail probability of $\frac{C}{I}$ and $\frac{C}{I+N}$ given by (2), for any SCS. Again, without loss of generality, we consider the 1-D SCS.

Theorem 3. *When shadow fading in the form of i.i.d non-negative random factors, $\{\Psi_i\}$, is introduced to 1-D SCS with BS density function $\lambda(r)$, such that the Ψ_i's are independent of the underlying Poisson point process of the 1-D SCS, the resulting system is equivalent to another 1-D SCS with a different BS density $\bar{\lambda}(r) = E_{\Psi}\left[\Psi^{\frac{1}{\varepsilon}}\lambda(\Psi^{\frac{1}{\varepsilon}}r)\right]$. Such an equivalence is valid as long as $E_{\Psi}\left[\Psi^{\frac{1}{\varepsilon}}\lambda(\Psi^{\frac{1}{\varepsilon}}r)\right] < \infty$.*

Proof: The proof is provided in Appendix C. ■

Further, the $\frac{C}{I}$ and $\frac{C}{I+N}$ at the MS in the 1-D SCS with shadow fading is the same as that in the equivalent 1-D SCS given in Theorem 3 where there is no shadow fading. Hence, using Theorem 1 and Corollary 6 on this equivalent 1-D SCS, we can find $\Phi_{\left(\frac{C}{I}\right)^{-1}}(\omega)$ and $\Phi_{\left(\frac{C}{I+N}\right)^{-1}}(\omega)$, respectively, and by plugging these into (7) and (17), the tail probability of $\frac{C}{I}$ and $\frac{C}{I+N}$ are computed. The following remarks are an immediate consequence of Theorem 3.

Remark 3. When shadow fading in the form of i.i.d non-negative random factors, $\{\Psi_i\}$, is introduced to a *homogeneous* l-D SCS with BS density λ_0, the resulting system is also a *homogeneous* l-D SCS with BS density $\lambda_0 \mathrm{E}_{\Psi}\left[\Psi^{\frac{l}{\varepsilon}}\right]$, as long as $\mathrm{E}_{\Psi}\left[\Psi^{\frac{l}{\varepsilon}}\right] < \infty$.

Remark 4. In a *homogeneous* l-D SCS with BS density λ_0,

(a) shadow fading has no effect on the $\frac{C}{I}$ at the MS (From Remark 3 and Remark 1), and,

(b) the effect of shadow fading is completely captured in the noise power term of the $\frac{C}{I+N}$ (From Remark 3 and Corollary 7).

Figure 2 shows that the tail probability of $\frac{C}{I}$ at the MS in a *homogeneous* l-D SCS with and without shadow fading are identical. Remark 4 provides a thoretical proof for this observation. Now, consider the following interesting example concerning log-normal shadow fading in a *homogeneous* l-D.

Example 1. Consider a *homogeneous* 2-D SCS with an average BS density λ_0, where each BS is affected by an i.i.d log-normal shadow fading factor which in dB has a mean 0 and standard deviation σ. Using Remark 3, the equivalent *homogeneous* 2-D SCS has a BS density $\bar{\lambda}_0 = \lambda_0 \exp\left(\frac{2\sigma^2}{\varepsilon^2}\right)$. Note that $\bar{\lambda}_0 \geq \lambda_0,\ \forall\ \sigma,\ \varepsilon$, and from Remark 4, the introduction of shadow fading actually improves the signal quality, measured in terms of $\frac{C}{I+N}$.

In the following section, we present a theorem that helps generalize the results for any arbitrary path-loss model.

VI. GENERALIZATION TO ARBITRARY PATH LOSS MODEL

So far, we have assumed the path loss model to be $\frac{1}{R^{\epsilon}}$. For some situations (like indoor channels), the path loss model could be different. However, the results in prior sections can still be applied if we transform an arbitrary path loss model to the canonical path loss model $\frac{1}{R}$ by the following theorem.

Theorem 4. *Let* $h(x),\ x \geq 0$*, be a monotonically increasing function with derivative* $h'(x) > 0$*,* $\forall\ x > 0$ *and inverse function* $h^{-1}(x)$*. the 1-D SCS with BS density function* $\lambda(r)$ *and path loss model* $\frac{1}{h(R)}$ *is equivalent to the 1-D SCS with a BS density function* $\bar{\lambda}(r) = \frac{\lambda(h^{-1}(r))}{h'(h^{-1}(r))}$ *and the canonical path loss model* $\frac{1}{R}$ *.*

Proof: Let $\bar{R} = h(R)$ be the equivalent BS location. Using the *Mapping Theorem* in [27], BS with locations $\bar{R}$ is also a Poisson point process, whose density is obtained below. For any non-homogeneous 1-D Poisson point process, $E\left[N\left(t+s\right) - N\left(t\right)\right] = \int_t^{t+s} \lambda(z)dz$ is the expected number of occurrences in the interval $(t, t+s)$. Thus,

$$\begin{aligned} E\left[N\left(r+s\right) - N\left(r\right)\right] &= E\left[\text{Number of BSs with } \bar{R} \in (r, r+s)\right] \\ &= E\left[\text{Number of BSs with } R \in \left(h^{-1}\left(r\right), h^{-1}\left(r+s\right)\right)\right] \\ &= \int_{z=h^{-1}(r)}^{h^{-1}(r+s)} \lambda\left(z\right) dz \;=\; \int_{z=r}^{r+s} \frac{\lambda\left(h^{-1}\left(z\right)\right)}{h'\left(h^{-1}\left(z\right)\right)} dz. \end{aligned}$$

Hence, the 1-D SCS with path-loss model $\frac{1}{h(R)}$ and a BS density function $\lambda(r)$ is equivalent to the 1-D SCS with path-loss model $\frac{1}{R}$ and BS density function $\bar{\lambda}\left(r\right)$. ■

Once the new BS density is found, all results in prior sections apply after setting $\varepsilon = 1$. For example, a *homogeneous* l-D SCS with path loss model $R^{-\varepsilon}$ is equivalent to the 1-D SCS with path loss model $\frac{1}{R}$ and BS density function, $\lambda'(r) = \frac{b_l}{\varepsilon} r^{\frac{l}{\varepsilon}-1}$. This explains why $\Phi_{\left(\frac{C}{I}\right)^{-1}}\left(\omega\right)$ in Corollary 3 is only a function of $\frac{l}{\varepsilon} - 1$.

In the following section, we present several applications of the theory developed so far, in studying important scenarios in wireless communications pertaining to cellular system, adhoc systems, multiple access techniques, cognitive radio technology and overlay of wireless networks.

VII. APPLICATIONS IN WIRELESS COMMUNICATIONS

Here, we study several scenarios in wireless communications by modeling the underlying system as a *homogeneous* l-D SCS with BS density λ_0, where $l = 1$ models the BS deployment along the highway, $l = 2$ models the planar deployments, and $l = 3$ corresponds to deployments in metropolitan and high-density residential areas.

Cellular Communications: So far, we have studied the signal quality at the MS in a cellular system where the signals from the BSs are affected by arbitrary path-loss and shadow fading. Several other situations besides these can also be studied. Firstly, transmission powers and the antenna gains, $\{K_i\}_{i=1}^{\infty}$, of all the BSs in the cellular system are seldom the same, in which case $\{K_i\}_{i=1}^{\infty}$ can be modelled as i.i.d. random variables with an appropriate distribution, independent of the underlying Poisson point process. By treating K_i's as shadow fading factors, their effect on the signal quality at the MS can be found. Moreover, all the remarks in Section V hold for K_i's as well. For example, consider the case where each BS has an ideal sectorized antenna with gain G and beam-width θ, such that BS's antenna faces the MS with probability $\frac{\theta}{2\pi}$, in which case $K_i = G$, and otherwise $K_i = 0$. In this case, from Theorem 3, $\overline{\lambda}_0 = \lambda_0 G^{\frac{2}{\varepsilon}} \frac{\theta}{2\pi}$ is the BS density of the equivalent *homogeneous* l-D SCS.

Multiple Access Techniques: Next, the signal quality at the MS in a cellular system employing different multiple access techniques can be studied. For example, in a code division multiple access (CDMA) system, the goal is to maintain a constant voice signal quality at the MS, which is done by power control. This goal is acheived by having the serving BS increase its transmission power by $\alpha = y\left(\frac{C}{I}\right)^{-1}$, where α is the power control factor or the processing gain, $\frac{C}{I}$ is the instantaneous signal quality at the MS, and y is the desired constant signal quality. In this formulation, α for each BS is a random variable and in general, the α's of nearby BSs are correlated. But if the correlation is small, the characteristic function of $\left(\frac{C}{I}\right)^{-1}$ computed in Section III-A enables radio designers to approximately model the power needs to communicate with a MS in a SCS. In another formulation, if α is a constant factor by which the power of the serving BS is improved, its effect on the tail probability $\frac{C}{I}$ at the MS is obtained by straightforward manipulations as $\mathbb{P}\left(\left\{\alpha\frac{C}{I} > y \middle| \varepsilon, l\right\}\right) = K_{\frac{\varepsilon}{l}}\left(\frac{y}{\alpha}\right)^{-\frac{l}{\varepsilon}}$ if $y > \alpha$.

Now, consider frequency division multiple access (FDMA) and time division multiple access (TDMA) based cellular systems. Let the available spectrum (in frequency for FDMA and in time-slots for TDMA) be divided into N parts called channel reuse groups (CG), and indexed as

$k = 1, 2, \cdots, N,$. Then, each BS is assigned one of the N CGs, such that the k^{th} CG is assigned with the probability p_k. In such a system, the MS chooses a CG that corresponds to the best $\frac{C}{I}$; the BS in the CG that corresponds to the strongest received power is the *desired* BS, and the MS chooses it as the serving BS. The $\frac{C}{I}$ at the MS in such a SCS is of interest to us. Note that this *homogeneous* l-D SCS is equivalent to N independent *homogeneous* l-D SCSs with constant BS densities $\lambda_0 p_1, \cdots, \lambda_0 p_N$, by the properties of Poisson point processes. The tail probability of $\frac{C}{I}$ at the MS in such a system is given by $\mathbb{P}\left(\left\{\frac{C}{I} > y \middle| \varepsilon, N\right\}\right) = 1 - \left[1 - \mathbb{P}\left(\left\{\frac{C}{I} > y \middle| \varepsilon\right\}\right)\right]^N$, where the tail probability on the right hand side is computed using Corollary 3 and (7).

Cognitive Radios: In cognitive radio technology, the cognitive radio devices (or *secondary users*) opportunistically operate in licensed frequency bands occupied by television (TV) transmitter-receiver pairs and wireless microphone systems (collectively called *primary users*). The interference caused by *secondary user* transmissions is harmful for *primary users* operation, and is not acceptable beyond certain limits. Studying the nature of these interferences and formulating methods for addressing them has been an active area of research. The results in this paper are a rich source of mathematical tools for such studies. In [30], we have extensively applied the results developed here, towards understanding the role of cooperation between the *secondary users* in ensuring that the interference caused by the *secondary users* are within the acceptable limits. The *secondary users* are modeled analogous to BS placement in *homogeneous* 1-D and 2-D SCS, and the tail probability of $\frac{C}{I}$ at the *primary user* is characterized. Further, in the context of radio environment map (REM, [30, and references therein]), we have highlighted the practical significance of the study of 1-D SCS. A more detailed account of the study of cognitive radio networks incorporating the results from this paper is a topic for future research.

Overlay Networks: The modern cellular communication network is a complex overlay of heterogeneous networks, such as macrocells, microcells, picocells and femtocells. This complex overlay network is seldom studied as is, due to the analytical intractabilities. In [2], [31], [32], cellular systems consisting of macrocell and femtocell networks are analyzed. Using the results in our paper, the cumulative effect of all the networks constituting the overlay network, on the signal quality at the MS can be studied. A detailed study on this is set aside as a future work.

VIII. CONCLUSIONS

In this paper, we comprehensively study the characterization of the $\frac{C}{I}$ and $\frac{C}{I+N}$ at the MS in the SCS where the SCS is defined as a cellular system where the BS deployment in a given region is according to a non-homogeneous Poisson point process. Analytical expressions for the tail probabilities of $\frac{C}{I}$ and $\frac{C}{I+N}$ at the MS are obtained for 1-D, 2-D and 3-D SCSs, where the 1-D, 2-D and 3-D SCS are mathematical models for BS deployments along the highway (1-D), in planar regions (2-D) and in metropolitan and residential areas (3-D), respectively. Further, a closed form expression for the tail probabilitiy of $\frac{C}{I}$ is derived for the homogeneous cases of 1-D, 2-D and 3-D SCS. Several mathematical tools are developed, that help in characterizing the instantaneous $\frac{C}{I}$ and $\frac{C}{I+N}$ at the MS when the MS is moving in the SCS. These results are applicable for general shadow fading distrubutions and arbitrary path-loss models. This makes the results directly applicable for analyzing many different wireless applications which are characterized by uncoordinated deployments. The application of this theory has been demonstrated in the study of the impact of cooperation between cognitive radios in the low power primary user detection and can be found in [30]. Future work will further explore the applications of the SCS model in the context of indoor femtocells, cognitive radios, and multi-tier or overlay networks.

APPENDIX

A. Useful Properties of 1-D SCS

In this section, some of the frequently used properties of the non-homogeneous Poisson point process in the context of 1-D SCS with BS density function $\lambda(r)$ are listed. Note that all the proofs are not provided here, and can be found in [22], [27], or in any of the elementary books on stochastic processes and Poisson processes.

Fact 1. *If R_1 denotes the separation of the serving BS from the MS, then, the p.d.f. of R_1, $f_{R_1}(r_1)$, is $f_{R_1}(r_1) = \lambda(r_1) \exp\left(-\int_{s=0}^{r_1} \lambda(s)\, ds\right), \ \forall\ r_1 \geq 0$.*

Fact 2. *If the BSs in the 1-D SCS are sorted in an ascending order of their distances from the MS denoted by random variables $R_1, R_2, \cdots$, then, the distance of the $(k-1)^{\text{th}}$ nearest*

BS from the MS is smaller in the usual stochastic order (Definition 4 in Section III-A1) *than the nearest* k^{th} *BS, i.e.* $R_{k-1} \leq_{st} R_k$*, and the p.d.f. of* R_k *conditioned on* R_{k-1} *is given by* $f_{R_k|R_{k-1}}(r_k|r_{k-1}) = \lambda(r_k)\exp\Big(-\int_{s=r_{k-1}}^{r_k}\lambda(s)ds\Big),\ \forall\ r_k \geq r_{k-1},\ k > 1.$

Fact 3. *When the separation of the* k^{th} *closest BS,* $R_k = r_k$*, the entire 1-D plane may be divided into 2 regions, namely,* $[0, r_k]$*and* (r_k, ∞)*. Any event in* $[0, r_k]$ *is independent of any event in* (r_k, ∞)*. Also, any event in non-overlapping intervals within the same region are independent of each other. The above statements follow from Definition 2.*

Lemma 3. *Let* $\{R_k\}_{k=1}^{\infty}$ *represent the set of distances of BSs from the MS (indexed in the ascending order of the distance),* $D_{k+1} = R_{k+1} - R_k$ *be the distance between two adjacent BSs, and* $f_{D_{k+1}|R_k}(d|\,r;\lambda(s))$ *be the p.d.f. of* D_{k+1} *conditioned on* $R_k = r$ *corresponding to the 1-D SCS with BS density* $\lambda(s),\ s \geq 0$*. Then,*

$$f_{D_{k+1}|R_k}(d\,|r;\lambda(s)) \;=\; e^{-\int_r^{r+d}\lambda(s)ds}\lambda(r+d),\ \text{and} \tag{19}$$

$$f_{aD_{k+1}|aR_k}(d'\,|r';\lambda(s)) \;=\; f_{D_{k+1}|R_k}\left(d'\,\middle|\,r';\frac{1}{a}\lambda(\frac{s}{a})\right). \tag{20}$$

Proof: The p.d.f. in (19) follows from Fact 2. Further, $f_{aD_{k+1}|aR_k}(d'|r';\lambda(s)) \overset{(a)}{=} \frac{1}{a}f_{D|R_k}\left(\frac{d'}{a}|\frac{r'}{a};\lambda(s)\right) \overset{(b)}{=} e^{-\int_{\frac{r'}{a}}^{\frac{r'+d'}{a}}\lambda(s)ds}\frac{1}{a}\lambda\left(\frac{r'+d'}{a}\right) \overset{(c)}{=} e^{-\int_{r'}^{r'+d'}\frac{1}{a}\lambda\left(\frac{s'}{a}\right)ds'}\frac{1}{a}\lambda\left(\frac{r'+d'}{a}\right)$, where (a) is obtained by expressing the p.d.f. in terms of D_{k+1} conditioned on R_k, (b) follows from (19), (c) is obtained by suitably manipulating the integral in the exponential, and finally, (20) is obtained from (c). ■

B. Proof of Theorem 1

We first derive the expression for the characteristic function of P_I conditioned on R_1, $\Phi_{P_I|R_1}(\omega|\,r_1)$, and use this to obtain the characteristic function of $\left(\frac{C}{I}\right)^{-1}$, $\Phi_{\left(\frac{C}{I}\right)^{-1}}(\omega)$.

Derivation for $\Phi_{P_I|R_1}(\omega|\,r_1)$*:* Consider a region $[0, R_B)$ in the 1-D plane such that $R_B \gg r_1$, and parition into $P1:\ [0, r_1]$ and $P2:\ (r_1, R_B)$. Next, partition $P2$ into N non-overlapping intervals $P2_j:\ \ (r_j = r_1 + (j-1)\Delta r, r_j + \Delta r = r_1 + j\Delta r)$, where $j = 1, 2, 3, \cdots, N$ and $\Delta r = \frac{R_B - r_1}{N}$. As $N \to \infty$, $\Delta r \to 0$ and it becomes unlikely for more than one BSs to exist in any partition $P2_j$. If X_j denotes the contribution to P_I by BSs in the j^{th} partition, then X_j

is a $\mathrm{Bernoulli}\,(p_j)$ random variable defined as $\mathbb{P}\left(\left\{ X_j = Kr_j^{-\varepsilon} + o\left(\Delta r\right) \middle| \, R_1 = r_1 \right\}\right) = p_j$, and $\mathbb{P}\left(\left\{ X_j = 0 \middle| \, R_1 = r_1 \right\}\right) = 1 - p_j$,where $p_j = \lambda(r_j)\Delta r + o(\Delta r)$ is the probability that there is exactly one BS in $P2_j, \ j = 1, 2, \cdots, N$. The characteristic of X_j is

$$\begin{aligned}
&\Phi_{X_j|R_1}\left(\omega|r_1\right) \overset{\text{(a)}}{=} \left(\lambda\left(r_j\right)\Delta r + o\left(\Delta r\right)\right) e^{i\omega\left(Kr_j^{-\varepsilon} + o(\Delta r)\right)} + 1 - \lambda\left(r_j\right)\Delta r + o\left(\Delta r\right) \\
&\overset{\text{(b)}}{=} 1 + \lambda\left(r_j\right)\Delta r\left(e^{i\omega Kr_j^{-\varepsilon}} - 1\right) + o(\Delta r) \overset{\text{(c)}}{=} 1 + \lambda\left(r_j\right)\Delta r\left(\sum_{k=1}^{\infty}\frac{\left(i\omega Kr_j^{-\varepsilon}\right)^k}{k!}\right) + o(\Delta r) \\
&\overset{(d)}{=} \exp\left(\lambda\left(r_j\right)\Delta r\left(\sum_{k=1}^{\infty}\frac{\left(i\omega Kr_j^{-\varepsilon}\right)^k}{k!}\right)\right) + o(\Delta r),
\end{aligned} \tag{21}$$

where (a) follows from the definition of the characteristic function, (b) is obtained by approximating the sum of two little-o functions with an equivalent little-o function, (c) is obtained by a Taylor's series expansion on the exponential function, and (d) is obtained by adding the necessary terms to form an exponential function and compensating for them in the little-o function.

Next, as $R_B \to \infty$, the total interference power is $P_I = \sum_{j=1}^{N} X_j$, where $\{X_j\}_{j=1}^{\infty}$ is a set of independent random variables, independent of R_1 due to our construction of $P1$, $P2$, and $P2_j, j = 1, 2, \cdots$ and Fact 3 in Appendix A. The characteristic function of P_I given $R_1 = r_1$ is

$$\begin{aligned}
\Phi_{P_I|R_1}\left(\omega|r_1\right) &= \lim_{R_B\to\infty}\lim_{\substack{N\to\infty \\ \Delta r\to 0}}\prod_{j=2}^{N}\Phi_{X_j|R_1}\left(\omega|r_1\right) \\
&= \lim_{R_B\to\infty}\lim_{\substack{N\to\infty \\ \Delta r\to 0}}\exp\left(\sum_{j=2}^{N}\left(\lambda\left(r_j\right)\Delta r\left(\sum_{k=1}^{\infty}\frac{\left(i\omega Kr_j^{-\varepsilon}\right)^k}{k!}\right)\right)\right) + o(\Delta r) \\
&= \lim_{R_B\to\infty}\exp\left(\int_{r=r_1}^{R_B}\lambda\left(r\right)\left(e^{i\omega Kr^{-\varepsilon}} - 1\right)dr\right) \\
&= \lim_{R_B\to\infty}\exp\left(\lim_{M\to\infty}\int_{r=r_1}^{R_B}\lambda\left(r\right)\sum_{n=1}^{M}\frac{\left(i\omega Kr^{-\varepsilon}\right)^n}{n!}dr\right) \\
&= \exp\left(\lim_{M\to\infty}\sum_{n=1}^{M}\frac{\left(i\omega K\right)^n}{n!}\lim_{R_B\to\infty}\int_{r=r_1}^{R_B}\lambda\left(r\right)r^{-n\varepsilon}dr\right).
\end{aligned}$$

Notice that $\Phi_{P_I|R_1}\left(\omega|r_1\right)$ exists if and only if $\lim\limits_{R_B\to\infty}\int_{r=r_1}^{R_B}\lambda(r)r^{-n\varepsilon}dr < \infty, \forall\, n \geq 1$ and $\forall\, r_1 > 0$, in which case $\Phi_{P_I|R_1}\left(\omega|r_1\right) = \exp\left(\sum_{n=1}^{\infty}\frac{(i\omega K)^n}{n!}\int_{r=r_1}^{\infty}\lambda\left(r\right)r^{-n\varepsilon}dr\right)$.

Derivation for $\Phi_{\left(\frac{C}{I}\right)^{-1}}(\omega)$*:* Firstly, recall that $\frac{C}{I} = \frac{P_S}{P_I}$ where $P_s = KR_1^{-\varepsilon}$, and $\Phi_{\left(\frac{C}{I}\right)^{-1}\big|R_1}(\omega|r_1) = \Phi_{P_I|R_1}\left(\frac{\omega}{P_S}\bigg| r_1\right)$. Hence, $\Phi_{\left(\frac{C}{I}\right)^{-1}}(\omega) = \mathrm{E}_{R_1}\left[\Phi_{\left(\frac{C}{I}\right)^{-1}\big|R_1}(\omega|R_1)\right]$ and (4) is obatined by simplifying the expression for $\Phi_{\left(\frac{C}{I}\right)^{-1}\big|R_1}(\omega|r_1)$. Lastly, $\lambda(r)$ should satisfy $\int_{s=0}^{r}\lambda(s)ds < \infty$, for the p.d.f. of R_1 in Fact 2 of Appendix A to exist.

Remark. The expression for the characteristic function can be derived from the characteristic functional of the Poisson point process in [27, Section 3.3, Page 31], but the proof technique presented here is emphasized, as it will be used in solving similar problems in the future.

C. *Proof of Theorem 3*

Let $\bar{R} = R\Psi^{-\frac{1}{\varepsilon}}$, where R is the random variable representing the distance from the MS to a BS in the 1-D SCS with a BS density function $\lambda(r)$, Ψ is the shadow fading factor corresponding to the BS, and $\bar{R}$ is the corresponding equivalent distance. Using the *product space representation* and *Marking Theorem* in [27], $\bar{R}$ also corresponds to the 1-D SCS with a BS density function derived below.

For any 1-D SCS, $E\left[N(t+s) - N(t)\right]$, the expected number of BSs in the interval $(t, t+s)$ is called the mean function and is given by $E\left[N(t+s) - N(t)\right] = \int_t^{t+s}\lambda(z)dz$. Let E[Number of BS in $\bar{R} \in (r, r+s)$] be denoted by $E\left[N(r+s) - N(r)\right]$. Then,

$$E\left[N(r+s) - N(r)\right] \overset{\text{(a)}}{=} \mathrm{E}_{\Psi}\left[\int_{\mathrm{r}\Psi^{\frac{1}{\varepsilon}}}^{(\mathrm{r+s})\Psi^{\frac{1}{\varepsilon}}}\lambda(\mathrm{z})\,\mathrm{dz}\right] \overset{(b)}{=} \int_{r}^{(r+s)} E_{\Psi}\left[\Psi^{\frac{1}{\varepsilon}}\lambda\left(z\Psi^{\frac{1}{\varepsilon}}\right)\right]dz,$$

where (a) is obtained by rewriting the expectation with respect to each realization of Ψ, and (b) is obtained by exchanging the order of integration and expectation in (b) as $E_{\Psi}\left[\Psi^{\frac{1}{\varepsilon}}\lambda\left(z\Psi^{\frac{1}{\varepsilon}}\right)\right] < \infty$. Hence, $\bar{R}'s$ corresponds to the 1-D SCS with a BS density function $\bar{\lambda}(r) = E_{\Psi}\left[\Psi^{\frac{1}{\varepsilon}}\lambda\left(r\Psi^{\frac{1}{\varepsilon}}\right)\right]$.

D. *Simulation Methods*

In this section, the details of simulating the SCS are presented. A single trial in simulating the BS placement for the 1-D SCS with BS density function $\lambda(r)$ in the region of interest which is a subset of the 1-D plane denoted by S, involves the following steps:

1) Generate a random number $M \sim \mathrm{Poisson}\left(\int_S \lambda\left(s\right) ds\right)$, which is the number of BSs to be placed in S for the given trial.

2) *BS placement:* For *homogeneous* 1-D SCS, generate M random numbers according to a uniform distribution in the range of S. If $\lambda(s)$ does not correspond to a *homogeneous* 1-D SCS, if $\lambda_{\max} = \sup\limits_{s \in S} \lambda(s)$, then general a random number $y \sim$ Uniform$(0, \lambda_{\max})$ and another random number x according to a uniform distribution in the range of S. A BS is placed uniformly at x, only if $y < \lambda_0(x)$. This process is repeated until M BS are placed.

3) Compute the received power at the MS for each BS using the path loss exponent ε. The shadow fading in the SCS is incorporated by multiplying each of the received powers with i.i.d. random number generated according to the distribution of the shadow fading factor. Finally, $\frac{C}{I}$ at the MS corresponding to this trial, is computed according to (2).

For all the simulations in this paper $T = 20000$ trials are used unless specified otherwise.

REFERENCES

[1] T. X. Brown, "Cellular performance bounds via shotgun cellular systems," *Selected Areas in Communications, IEEE Journal on*, vol. 18, pp. 2443–2455, Nov 2000.

[2] V. Chandrasekhar and J. Andrews, "Uplink capacity and interference avoidance for two-tier femtocell networks," *Wireless Communications, IEEE Transactions on*, vol. 8, pp. 3498 –3509, July 2009.

[3] J. G. Andrews, N. Jindal, M. Haenggi, R. Berry, S. Jafar, D. Guo, S. Shakkottai, R. W. H. Jr., M. Neely, S. Weber, and A. Yener, "Rethinking information theory for mobile ad hoc networks," *IEEE Communications Magazine*, vol. 46, pp. 94–101, December 2008.

[4] A. M. Hunter, J. G. Andrews, and S. Weber, "Capacity scaling laws for ad hoc networks with spatial diversity," in *Proceedings of the IEEE International Symposium on Information Theory (ISIT)*, (Nice, France), June 2007.

[5] A. M. Hunter, J. G. Andrews, and S. Weber, "Capacity scaling of ad hoc networks with spatial diversity," *IEEE Transactions on Wireless Communications*, vol. 7, pp. 5058–5071, December 2008.

[6] N. Jindal, J. G. Andrews, and S. Weber, "Energy-limited vs. interference-limited ad hoc network capacity (invited)," in *Proceedings of the 41st Annual Asilomar Conference on Signals, Systems, and Computers*, (Pacific Grove, CA), November 2007.

[7] K. T. Truong, S. Weber, and R. W. H. Jr., "Transmission capacity of two-way communication in wireless ad hoc networks," in *Proceedings of the International Conference on Communications (ICC)*, (Dresden, Germany), June 2009.

[8] S. Weber, J. G. Andrews, X. Yang, and G. de Veciana, "Transmission capacity of CDMA ad hoc networks employing successive interference cancellation," in *Proceedings of the 47th annual IEEE Global Telecommunications Conference (Globecom)*, (Dallas, TX), November 2004.

[9] S. Weber, J. G. Andrews, X. Yang, and G. de Veciana, “Wireless ad hoc networks with successive interference cancellation,” in *Proceedings of the 43rd annual Allerton conference on communication, control, and computing*, (Monticello, IL), September 2005.

[10] S. Weber and J. G. Andrews, “A stochastic geometry approach to wideband ad hoc networks with channel variations,” in *Proceedings of the Second Workshop on Spatial Stochastic Models for Wireless Networks (SPASWIN)*, (Boston, MA), April 2006.

[11] S. Weber, X. Yang, G. de Veciana, and J. Andrews, “Transmission capacity of CDMA ad-hoc networks,” in *Spread Spectrum Techniques and Applications, 2004 IEEE Eighth International Symposium on*, pp. 245–249, 2004.

[12] S. Weber, X. Yang, J. G. Andrews, and G. de Veciana, “Transmission capacity of wireless ad hoc networks with outage constraints,” *IEEE Transactions on Information Theory*, vol. 51, pp. 4091–4102, December 2005.

[13] J. Wildman, D. Hamel, R. Measel, D. Oakum, S. Weber, and M. Kam, “Performance and scaling of wireless ad hoc IPv6 stateless address autoconfiguration under mobile gateways,” in *Proceedings of the Military Communications Conference (MILCOM)*, (Orlando, FL), October 2007.

[14] S. Weber, J. G. Andrews, and N. Jindal, “Throughput and transmission capacity of ad hoc networks with channel state information,” in *Proceedings of the 44th Annual Allerton Conference on Communication, Control, and Computing*, (Monticello, IL), September 2006.

[15] S. Weber and J. G. Andrews, “Transmission capacity of wireless ad hoc networks with channel variations,” in *Proceedings of the 40th Annual Asilomar Conference on Signals, Systems, and Computers*, (Pacific Grove, CA), October 2006.

[16] S. Weber, X. Yang, G. de Veciana, and J. G. Andrews, “Transmission capacity of CDMA ad-hoc networks,” in *Proceedings of the 8th IEEE International Symposium on Spread Spectrum Techniques and Applications (ISSSTA)*, (Sydney, Australia), August 2004.

[17] J. G. Andrews, S. Weber, and M. Haenggi, “Ad hoc networks: to spread or not to spread?,” *IEEE Communications Magazine*, vol. 45, pp. 84–91, December 2007.

[18] N. Jindal, S. Weber, and J. G. Andrews, “Fractional power control for decentralized wireless networks,” *IEEE Transactions on Wireless Communications*, vol. 7, pp. 5482–5492, December 2008.

[19] N. Jindal, J. G. Andrews, and S. Weber, “Bandwidth partitioning in decentralized wireless networks,” *IEEE Transactions on Wireless Communications*, vol. 7, pp. 5408–5419, December 2008.

[20] H. Takagi and L. Kleinrock, “Optimal transmission ranges for randomly distributed packet radio terminals,” *Communications, IEEE Transactions on*, vol. 32, pp. 246–257, Mar 1984.

[21] M. Zorzi and S. Pupolin, “Outage probability in multiple access packet radio networks in the presence of fading,” *Vehicular Technology, IEEE Transactions on*, vol. 43, pp. 604–610, Aug 1994.

[22] S. M. Ross, *Stochastic Processes*. John Wiley & Sons, Inc., 1983.

[23] D. Cox, “Universal digital portable radio communications,” *Proceedings of the IEEE*, vol. 75, pp. 436–477, April 1987.

[24] T. S. Rappaport, *Wireless Communications: Principles and Practice*. Upper Saddle River, NJ, USA: Prentice-Hall, Inc., 1996.

[25] P. Madhusudhanan, J. G. Restrepo, Y. E. Liu, and T. X. Brown, “Carrier to interference ratio analysis for the shotgun cellular system,” in *IEEE Globecom 2009 Wireless Communications Symposium*, (Honolulu, HI, USA), November 2009.

[26] M. Shaked and J. G. Shanthikumar, *Stochastic Orders*. Springer, 2006.

[27] J. F. C. Kingman, *Poisson Processes (Oxford Studies in Probability)*. Oxford University Press, USA, January 1993.

[28] A. M. Mathai and H. J. Haubold, *Special Functions for Applied Scientists*. Springer, March 2008.

[29] T. X. Brown, “Analysis and coloring of a shotgun cellular system,” *Radio and Wireless Conference, 1998. RAWCON 98. 1998 IEEE*, pp. 51–54, Aug 1998.

[30] P. Madhusudhanan, J. G. Restrepo, Y. Liu, T. X. Brown, and K. Baker, “Modeling of interference from cooperative cognitive radios for low power primary users,” in *IEEE Globecom 2010 Wireless Communications Symposium*, pp. 1–6, 2010.

[31] P. Xia, V. Chandrasekhar, and J. Andrews, “Cdma uplink capacity in both open and closed access two-tier femtocell networks,” in *GLOBECOM Workshops (GC Wkshps), 2010 IEEE*, pp. 648 –652, 2010.

[32] P. Xia, V. Chandrasekhar, and J. Andrews, “Open vs. closed access femtocells in the uplink,” *Wireless Communications, IEEE Transactions on*, vol. 9, no. 12, pp. 3798 –3809, 2010.

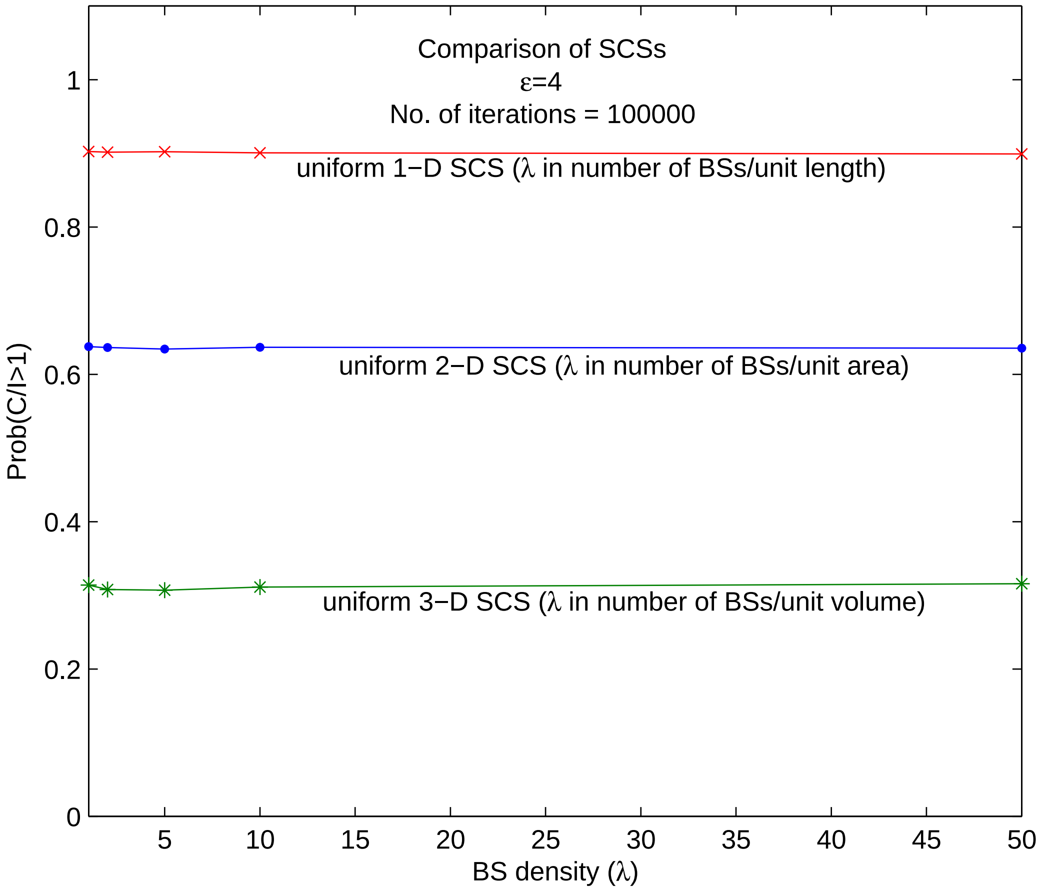

Figure 1. Invariance of the performance of homogeneous l-D SCS on the BS density.

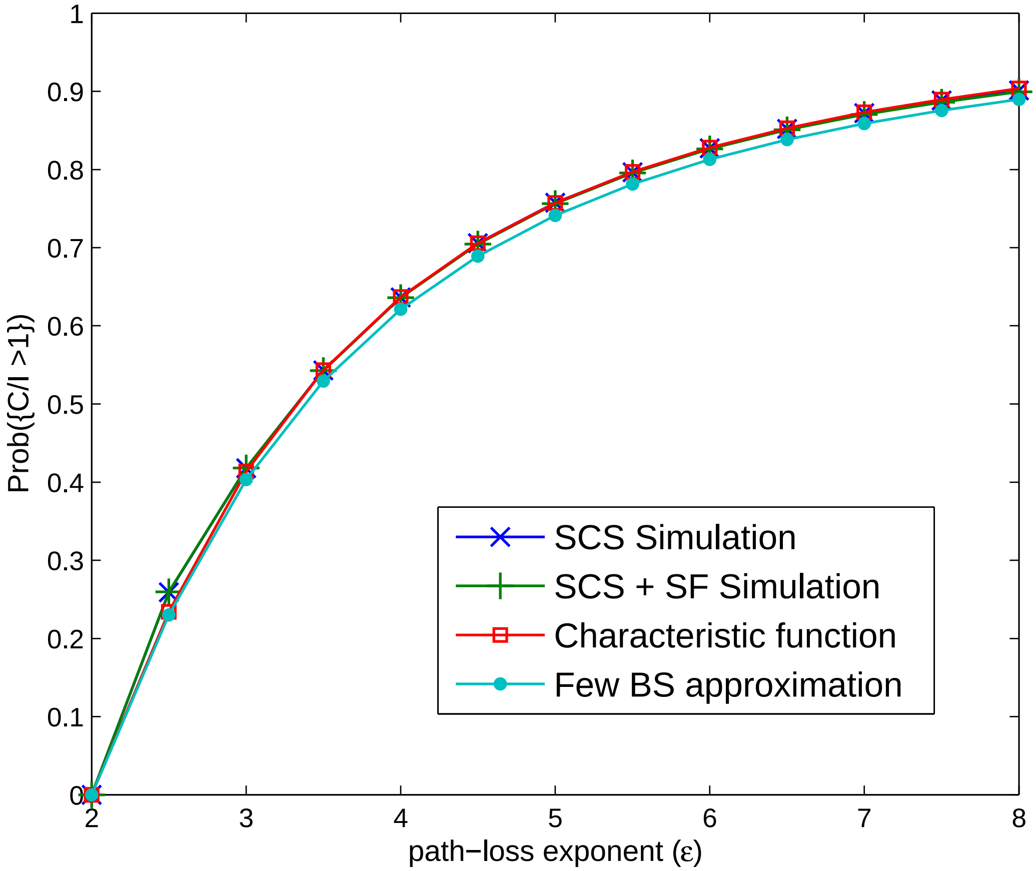

Figure 2. Comparison of Simulations with the analytical results

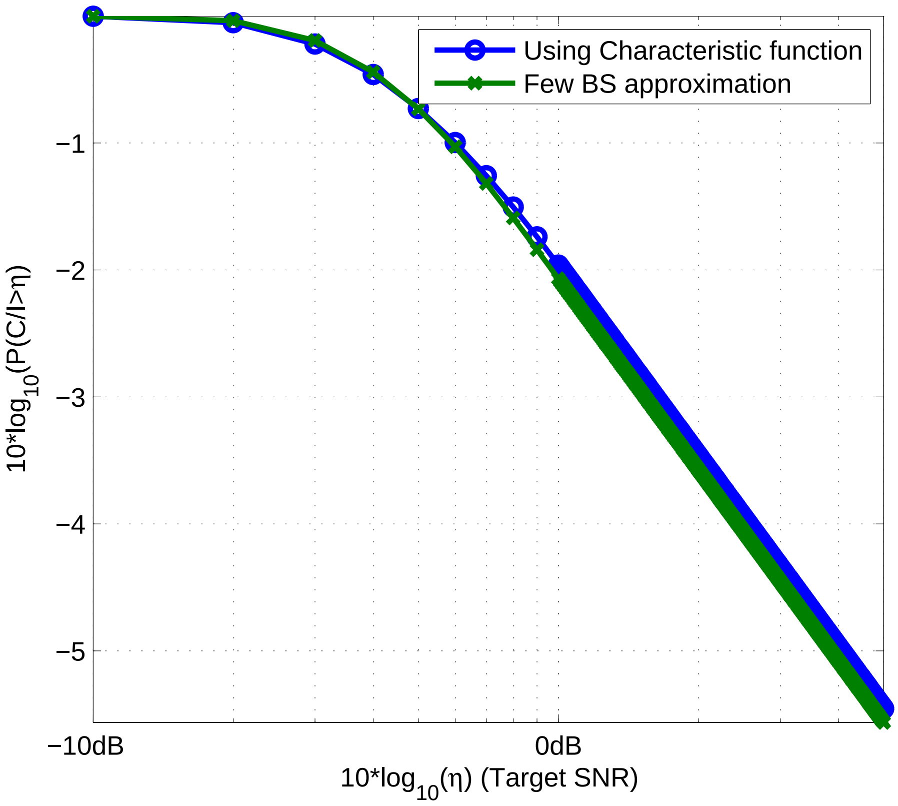

Figure 3. Homogeneous 2-D SCS: Comparing $\frac{C}{I}$ and $\frac{C}{I_2}$, $\varepsilon = 4$

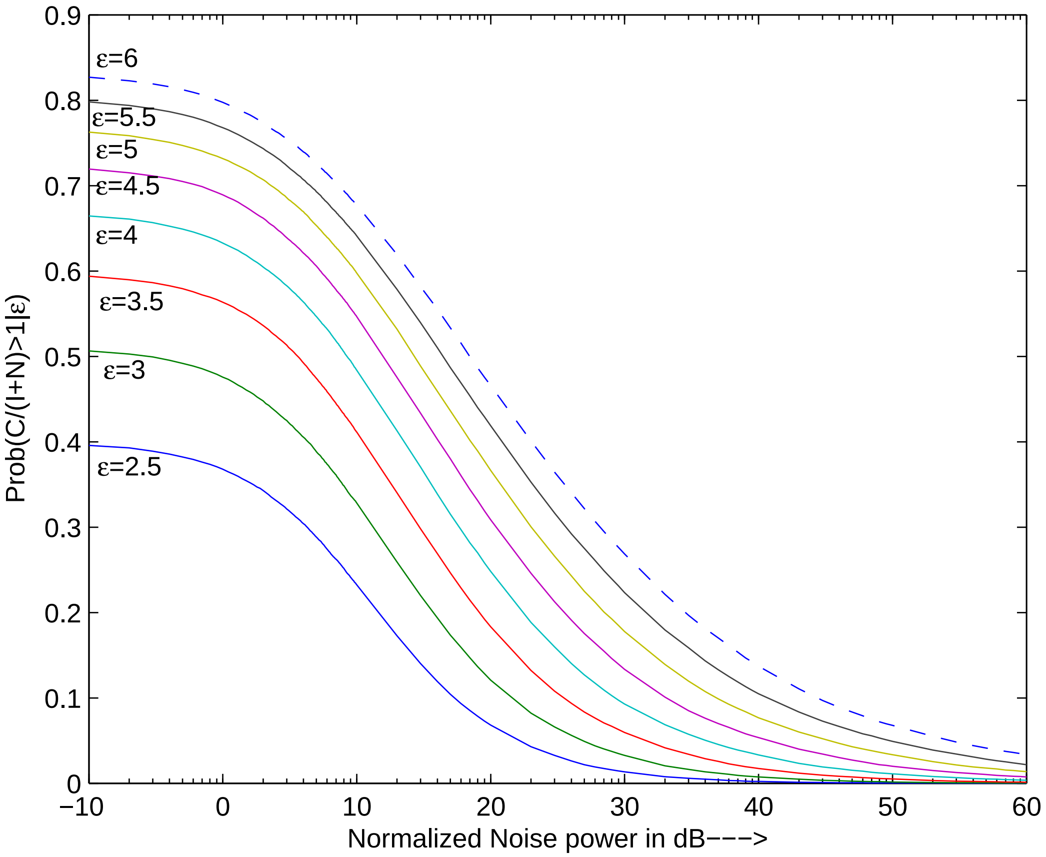

Figure 4. Plot of $\mathrm{Prob}\left(\left\{\frac{C}{I+N} > 1\right\}\right)$ vs Noise power